

<b>REPORT DOCUMENTATION PAGE</b>			Form Approved OMB NO. 0704-0188		
<p>The public reporting burden for this collection of information is estimated to average 1 hour per response, including the time for reviewing instructions, searching existing data sources, gathering and maintaining the data needed, and completing and reviewing the collection of information. Send comments regarding this burden estimate or any other aspect of this collection of information, including suggestions for reducing this burden, to Washington Headquarters Services, Directorate for Information Operations and Reports, 1215 Jefferson Davis Highway, Suite 1204, Arlington VA, 22202-4302. Respondents should be aware that notwithstanding any other provision of law, no person shall be subject to any penalty for failing to comply with a collection of information if it does not display a currently valid OMB control number.</p> <p>PLEASE DO NOT RETURN YOUR FORM TO THE ABOVE ADDRESS.</p>					
1. REPORT DATE (DD-MM-YYYY) 26-02-2019		2. REPORT TYPE Final Report		3. DATES COVERED (From - To) 30-Sep-2017 - 30-Nov-2018	
4. TITLE AND SUBTITLE Final Report: New Principles for Targeting and Triggering based on Molecular Self-Assembly in Topological Defects of Liquid Crystals			5a. CONTRACT NUMBER W911NF-17-1-0575		
			5b. GRANT NUMBER		
			5c. PROGRAM ELEMENT NUMBER 611102		
6. AUTHORS			5d. PROJECT NUMBER		
			5e. TASK NUMBER		
			5f. WORK UNIT NUMBER		
7. PERFORMING ORGANIZATION NAMES AND ADDRESSES University of Wisconsin - Madison Suite 6401 21 N Park Street Madison, WI 53715 -1218			8. PERFORMING ORGANIZATION REPORT NUMBER		
9. SPONSORING/MONITORING AGENCY NAME(S) AND ADDRESS (ES) U.S. Army Research Office P.O. Box 12211 Research Triangle Park, NC 27709-2211			10. SPONSOR/MONITOR'S ACRONYM(S) ARO		
			11. SPONSOR/MONITOR'S REPORT NUMBER(S) 71259-CH.7		
12. DISTRIBUTION AVAILABILITY STATEMENT Approved for public release; distribution is unlimited.					
13. SUPPLEMENTARY NOTES The views, opinions and/or findings contained in this report are those of the author(s) and should not be construed as an official Department of the Army position, policy or decision, unless so designated by other documentation.					
14. ABSTRACT					
15. SUBJECT TERMS					
16. SECURITY CLASSIFICATION OF:			17. LIMITATION OF ABSTRACT UU	15. NUMBER OF PAGES	19a. NAME OF RESPONSIBLE PERSON Manos Mavrikakis
a. REPORT UU	b. ABSTRACT UU	c. THIS PAGE UU			19b. TELEPHONE NUMBER 608-262-9053

**RPPR Final Report**  
as of 28-May-2019

Agency Code:

Proposal Number: 71259CH

**Agreement Number: W911NF-17-1-0575**

**INVESTIGATOR(S):**

**Name:** Manos Mavrikakis  
**Email:** manos@engr.wisc.edu  
**Phone Number:** 6082629053  
**Principal:** Y

**Name:** Nathan C. Gianneschi  
**Email:** nathan.gianneschi@northwestern.edu  
**Phone Number:** 8474671802  
**Principal:** N

Organization: **University of Wisconsin - Madison**

Address: Suite 6401, Madison, WI 537151218

Country: USA

DUNS Number: 161202122

EIN: 396006492

**Report Date:** 28-Feb-2019

Date Received: 26-Feb-2019

**Final Report** for Period Beginning 30-Sep-2017 and Ending 30-Nov-2018

**Title:** New Principles for Targeting and Triggering based on Molecular Self-Assembly in Topological Defects of Liquid Crystals

**Begin Performance Period:** 30-Sep-2017

**End Performance Period:** 30-Nov-2018

**Report Term:** 0-Other

Submitted By: Ph.D. Nicholas Abbott

Email: nla34@cornell.edu

Phone: (607) 255-3601

**Distribution Statement:** 1-Approved for public release; distribution is unlimited.

**STEM Degrees:** 0

**STEM Participants:** 4

**Major Goals:** Molecular self-assembly in aqueous systems arises from a delicate interplay of entropic and enthalpic effects associated with the structuring of water. This interplay also underlies many of the remarkable macroscopic material responses to molecular cues that are encountered in biological systems. Recently, new insight into self-assembly of amphiphilic molecules in an alternative class of structured solvents, specifically nematic solvents, has been reported. The presence of long-range orientational order in nematic solvents was shown to open new avenues to control of molecular assemblies that are not possible in aqueous systems. One key opportunity revolves around the formation of topological defects in nematic solvents, which can serve as virtual templates for triggering and hosting molecular assemblies. Motivated by these observations, this proposal seeks to develop a fundamental understanding of equilibrium and dynamic aspects of molecular self-assembly of amphiphiles in defects of nematic solvents, and to leverage that understanding to demonstrate principles that permit formation of single nanoscopic assemblies to be amplified into macroscopic outputs.

The approach described in this proposal builds from recent observations by PI Abbott that the nanoscopic cores of topological defects formed in nematic solvents, which are molecularly disordered relative to bulk nematic solvents, selectively trigger cooperative self-assembly of amphiphiles. These observations generate a range of questions regarding the equilibrium and dynamic properties of these assemblies, the answers to which will enable development of new principles for amplification of signals across multiple time and length scales. The research is organized into three parts. First, experiments will be performed to provide insight into the thermodynamics of molecular self-assembly in topological defects, including the relationship between amphiphile molecular structure and assembly morphology, and the role of entropy and enthalpy in driving self-assembly. The experiments will be enabled by synthesis of families of polymeric amphiphiles by reversible addition fragmentation chain transfer (RAFT) and ring-opening metathesis polymerization (ROMP) in the research group of co-PI Gianneschi. Second, the coupling between dynamics of molecular self-assembly and dynamics of defect motion will be elucidated, building on the preliminary observation that macroscopic dynamics of defects can report formation of a single nanoscopic amphiphilic assembly. A key aspect will be synthesis of amphiphiles with tailored dynamics using ROMP and RAFT. Third, we will design amphiphilic polymers that can be triggered (e.g., by light) to undergo self-assembly in defects, and in doing so, generate macroscopic changes in the dynamic and equilibrium organization

## RPPR Final Report as of 28-May-2019

of nematic liquid crystalline systems that can be observed visually. This goal will integrate a new approach for preparing ROMP-based amphiphilic polymers that uses a light-activated ruthenium catalyst.

In summary, this project will advance our understanding of molecular self-assembly in nematic solvents and offers the potential to provide new principles that lead to macroscopic responses from molecular cues. The focus is fundamental, but the long-term impact of the research has the potential to guide new designs of triggerable and responsive soft materials of broad utility to DoD, including for (i) amplification of molecular events into the optical scale, (ii) design of sentient materials, and (iii) interfacial designs of chemical and biological sensors.

**Accomplishments:** Please see attached PDF

**Training Opportunities:** This project provided training opportunities for graduate students and postdoctoral researchers to participate in multi-disciplinary and multi-institutional research. Regular teleconferences and in-person discussions provide graduate students in chemical engineering (UW Madison) with the opportunity to work with postdoctoral researchers from chemistry (Northwestern). Undergraduate researchers were also integrated into both research groups, providing opportunities for undergraduates to understand the purposes and processes of research.

**Results Dissemination:** Abbott and Gianneschi gave a number of invited lectures:

Abbott, N. L., Reilly Lectures, University of Notre Dame, April 2018 Abbott, N.L.,  
Patten Lecture, U of Colorado, Boulder, May 2018  
Abbott, N.L., Chemical Engineering Seminar, Ohio State University, February 2018 Abbott, N.L., Invited Talk,  
APS March Meeting, LA, March 2018  
Abbott, N.L., Invited Talk, Int. Association of Coll and Interface Science, Rotterdam, May, 2018 Abbott, N.L.,  
Plenary Lecture, International Liquid Crystal Conference, Kyoto, July, 2018

Gianneschi, N. C. Invited Lecture, UC Irvine, January 2018 Gianneschi, N.C. Invited Lecture, Indiana University,  
February 2018  
Gianneschi, N. C. Invited Lecture, Max Planck Institute for Polymer Research, February 2018

**Honors and Awards:** 2018 Lectureship Award of Division of Colloid and Surface Chemistry, Chemical Society of Japan.  
2018 Tisch University Professorship, Cornell University  
2018 Patten Distinguished Lecture, University of Colorado-Boulder  
2018 Reilly Lectures, University of Notre Dame

**Protocol Activity Status:**

**Technology Transfer:** Nothing to report

Nicholas Abbott participated in an army-sponsored workshop at Natick in the fall of 2018. The workshop focused on integration of antimicrobial functionality into materials, including fabrics.

### PARTICIPANTS:

**Participant Type:** PD/PI

**Participant:** Nicholas Lawrence Abbott

**Person Months Worked:** 1.00

Project Contribution:

International Collaboration:

International Travel:

National Academy Member: Y

Other Collaborators:

**Funding Support:**

**Participant Type:** Co PD/PI

**Participant:** Nathan Gianneschi

**RPPR Final Report**  
as of 28-May-2019

**Person Months Worked:** 1.00

**Funding Support:**

Project Contribution:

International Collaboration:

International Travel:

National Academy Member: N

Other Collaborators:

**Participant Type:** Postdoctoral (scholar, fellow or other postdoctoral position)

**Participant:** Daniel Wright

**Person Months Worked:** 8.00

**Funding Support:**

Project Contribution:

International Collaboration:

International Travel:

National Academy Member: N

Other Collaborators:

**Participant Type:** Postdoctoral (scholar, fellow or other postdoctoral position)

**Participant:** Karthik Nayani

**Person Months Worked:** 8.00

**Funding Support:**

Project Contribution:

International Collaboration:

International Travel:

National Academy Member: N

Other Collaborators:

**Participant Type:** Graduate Student (research assistant)

**Participant:** Womin Choi

**Person Months Worked:** 8.00

**Funding Support:**

Project Contribution:

International Collaboration:

International Travel:

National Academy Member: N

Other Collaborators:

**Participant Type:** Graduate Student (research assistant)

**Participant:** Kevin Zeng

**Person Months Worked:** 6.00

**Funding Support:**

Project Contribution:

International Collaboration:

International Travel:

National Academy Member: N

Other Collaborators:

**RPPR Final Report**  
as of 28-May-2019

## Final Report - Technical Progress

Molecular self-assembly in aqueous systems arises from a delicate interplay of entropic and enthalpic effects associated with the structuring of water. This project is developing new insight into self-assembly of amphiphilic molecules in an alternative class of structured solvents, specifically nematic solvents. The project is showing that the presence of long-range orientational order in nematic solvents opens new avenues to control of molecular assemblies that are not possible in aqueous systems, including *formation of topological defects in nematic solvents as virtual templates for triggering and hosting molecular assemblies*. Over the past year, we have performed experiments to provide insight into the thermodynamics of molecular self-assembly in topological defects of liquid crystals, including the relationship between amphiphile molecular structure and assembly morphology, and the role of entropy and enthalpy in driving self-assembly. The experiments have been made possible by advances in the development of a new experimental system that generates well-defined defects in liquid crystals (Abbott), and by the synthesis of families of polymeric amphiphiles by reversible addition fragmentation chain transfer (RAFT) (Gianneschi). In addition, we have performed measurements of the coupling between dynamics of molecular self-assembly and dynamics of defect motion, building evidence that the macroscopic dynamics of defects can report formation of a single nanoscopic amphiphilic assembly (Abbott). Below we summarize key elements of this progress.

### Development of a new experimental system to generate topological defects in liquid crystals.

As noted above, a key goal of our project is to develop an understanding of molecular self-assembly of amphiphiles templated from topological defects in liquid crystals. In our past experimental studies, we generated defects by dispersing silica microparticles, treated with octyltrichlorosilane, in an isotropic phase of 4-cyano-4'-pentylbiphenyl (5CB) that contained a predetermined concentration of amphiphile (BODIPY-C5). The surface treatment of the microparticles promoted perpendicular anchoring of the nematic liquid crystals. The particle-liquid crystal mixture was introduced in the isotropic state between two glass substrates that were polyimide-coated, unidirectionally rubbed, and oriented 90° relative to one another, thereby inducing twist within the nematic phase upon cooling (Fig. 1). In the presence of the surface-treated particles, the combined boundary conditions yield a singular line defect of strength  $-1/2$  around and between the particles. This procedure readily produces line defects, but limits the long-term study of defects because the lengths of the defect lines change over time as particles migrate in the liquid crystal medium. Typically, the distance between particles shortens over time to reduce the lengths of the defects and minimize the free energy of the system. This relaxation of the defects over time made quantitative characterization of self-assembly of molecules within the defects challenging and motivated efforts pursued over the past year to generate better defined defects.

To address the above-described limitation of our prior experimental approach, over the past year, we developed a new system for studying self-assembly in topological defects. As shown in Fig. 1b, two metallic wires were introduced between two planar glass substrates. Both the wires and the glass substrates were treated with dimethyloctadecyl[3-(trimethoxysilyl)propyl]ammonium (DMOAP) to induce perpendicular anchoring of nematic liquid crystals at their surfaces. These boundary conditions cause the director field of the liquid crystal to bend and generate two line

defects of strength  $-1/2$ , satisfying the topology of the confined nematic domain. As drawn in Fig. 1b, the director is locked perpendicular to the two glass substrates, while the director bends upon approaching the wires. The resulting defect lines run parallel to the surfaces of the wires, as shown by the red defect (disclination) cores in Fig 1b. Since the boundary condition is defined by stationary elements, we found that the new system reliably creates  $-1/2$  disclinations, avoiding issues associated with microparticles freely dispersed in liquid crystals in our previous setup. Additionally, we confirmed that the generated disclinations were stable over three weeks.

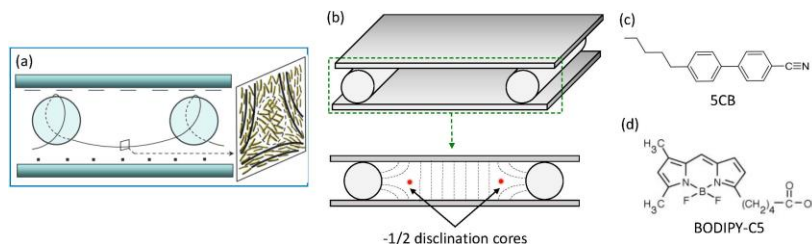


**Figure 1. Experimental designs and materials.** (a) The original design for generating a  $-1/2$  line defect (disclination) by adding microparticles to a nematic liquid crystal (reproduced from [1]). (b) New experimental design of optical cells for creating  $-1/2$  disclinations that are running parallel to the wires. (c-d) Molecular structures of compounds; (c) a nematic liquid crystal (5CB) and (d) dipyrrometheneborondifluoride (BODIPY)-labelled amphiphile.

### Self-assembly of BODIPY-C5 amphiphiles in topological defects induced by wires

Using the above-described system, we have performed measurements of self-assembly in topological defects of 5CB (Fig. 2). The experimental procedure involved introducing an isotropic mixture of 5CB and BODIPY-C5 into the newly designed optical cell. As the mixture was cooled to the nematic phase, the boundary conditions cause singular disclinations to be formed approximately  $30\text{--}40\text{ }\mu\text{m}$  from the surface of the wires (for  $300\text{ }\mu\text{m}$ -diameter wires). As noted above, the direction of the disclinations (defect lines) is parallel to the long axes of the wires. The line defects are millimeters in length and both ends anchor on the wire surface. Optical microscopy can readily image the defects because the core of the defects scatter light (Fig. 2b) and because the orientation of the liquid crystals varies abruptly in close proximity to each defect core.

We imaged fluorescently-labeled (i.e., BODIPY-labeled) amphiphiles to observe their self-association behavior in defects. The fluorescence emission of the BODIPY group changes depending on whether it is singly dispersed or self-assembled; measurement of fluorescent emissions using  $\lambda^{\text{excitation}} = 533\text{--}584\text{ nm}$  and  $\lambda^{\text{emission}} = 606\text{--}684\text{ nm}$  indicates self-association of the amphiphiles. When using  $70\text{ }\mu\text{M}$  BODIPY-C5 in 5CB, fluorescence microscopy (Fig. 2c) revealed that the amphiphiles are assembled in the defect (intense fluorescence along the disclination). This result suggests that the critical aggregation concentration of the BODIPY-C5 is less than  $70\text{ }\mu\text{M}$  in the environment of the  $-1/2$  defect. Additionally, we observed some bright spots (dimer emission) in the left part of the image, indicating that there is some extent of aggregation of the BODIPY-C5 amphiphile at this concentration in the bulk of the nematic liquid crystal. It is possible that these aggregates reflect the presence of dust or other impurities in the sample – additional measurements are needed to establish the origin of these features in the images. Overall, however, measurements such as these have established the feasibility of using this new experimental system for studies of self-assembly in defects. In addition to these measurements, we have performed measurements of self-assembly as a function of temperature (to explore

entropic and enthalpic contributions to the driving force for self-assembly), and also using lipids with alternative architectures (as described in the proposal). The analysis of these measurements and others is underway.

### Self-assembly of BODIPY-labeled polymers synthesized using RAFT

As described in the introduction to this progress report, a key goal of this project is to synthesize amphiphilic polymers, and through systematic variation in the structure of the polymers, develop structure-property

relationships for self-assembly of amphiphiles in defects. Specifically, we hypothesized that the length of the aliphatic side chains of amphiphiles regulates a key part of the driving force for self-assembly of amphiphiles in defects of liquid crystals. Accordingly, over the past year, we have explored the self-assembly behavior of BODIPY-labelled polymers with side-chains that vary in length to systematically manipulate the forces driving self-assembly in defects. Specifically, enabled by the participation of the Gianneschi group in this project, we synthesized amphiphilic polymers with varying side chain functionality, including aromatic (poly(styrene)) or aliphatic (poly(butyl acrylate)) polymer side chains (**Figure 3**). The polymer systems were synthesized via Reversible Addition-Fragmentation chain Transfer (RAFT). The chain transfer agent chosen was 2-(dodecylthiocarbonothioylthio)-2-methylpropionic acid, which offers good control of the polymerization yet affords the polymers with a free carboxylic acid functional group. This carboxylic acid functional group was further modified via esterification with a hydroxy functionalized BODIPY dye to form BODIPY labelled polymers. Initially, polymers were targeted to have a degree of polymerization (DP) of 25, with the goal of providing sufficient block length to drive assembly in the defect yet not too large of a block to lead to aggregation in the bulk of the liquid crystal.

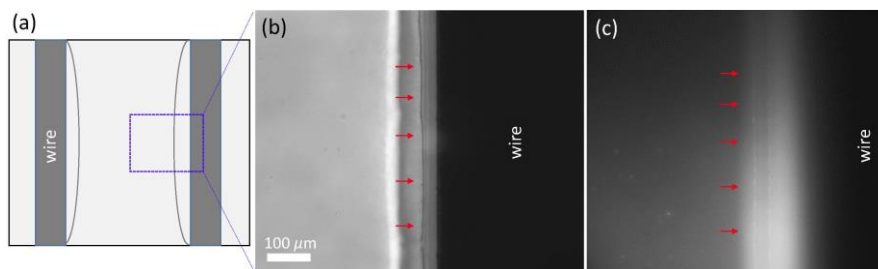


**Figure 2. Disclination lines and self-assembly of amphiphiles in a line defect.** (a) Schematic illustration of two  $-1/2$  line defects generated by the boundary conditions and anchored on the wires. (b) Optical micrograph of a line defect (indicated by red arrows) and (c) Fluorescence micrograph ( $\lambda_{\text{excitation}}$  533-584 nm,  $\lambda_{\text{emission}}$  606-684 nm) showing the selectively assembled amphiphiles in the disclination through the intense fluorescence (indicated by red arrows).

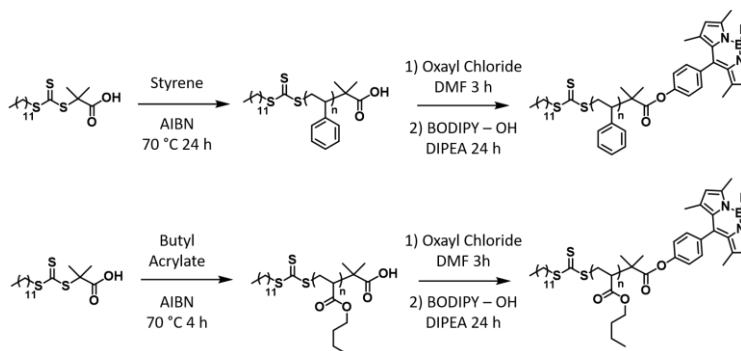


**Figure 3.** Schematic of the synthesis of the BODIPY end group functionized poly(styrene) and poly(butyl acrylate) by RAFT.

Similar to the BODIPY-C5 molecule shown in Figure 2, the incorporation of the BODIPY dye into the polymers allows for liquid crystal defect assembly to be elucidated via measurements of fluorescence. In an initial survey study, the assembly of either poly(styrene) or poly(butyl acrylate) was investigated, where it was deduced that the poly(butyl acrylate) exhibited a much enhanced tendency to undergo self-assembly in the defects of 5CB than the poly(styrene). Therefore, subsequent poly(alkyl acrylates) were synthesized via RAFT to investigate the role of the side chain length. For these new polymers, the block length remained constant, but the length of the aliphatic side chain increased in length, specifically we explored hexyl acrylate (C6 side chain length) and lauryl acrylate (C12 side chain length). Additional characterization was undertaken on the polymer samples using size exclusion chromatography with a UV detector (SEC-UV). The combination of the two analytical methods established labelling of the polymer side chain when the UV detector is set to the  $\text{Abs}_{\text{Max}}$  of BODIPY. Figure 4 shows an example with poly(butyl acrylate), confirming overlap of the signal from UV and light scattering traces. Figure 5 shows the structures of the three poly(alkyl acrylates), with different aliphatic chain lengths, that we have investigated.

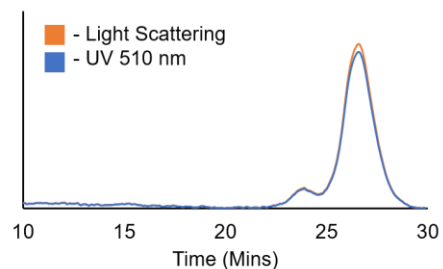


**Figure 4.** Poly(butyl acrylate), showing both UV and light scattering traces overlapping.

Prior to performing experiments involving the self-assembly of these polymers, we characterized further their absorbance and fluorescence properties. These measurements have identified some unanticipated observations that ongoing experiments are seeking to resolve. Specifically, as shown in Figure 6, we observe the absorbance and fluorescence properties of these polymers in both 5CB and chloroform to be non-monotonic with length of the alkyl side chain of these polymers. We are currently working to determine if this indicates some chain-length dependent difference in their dispersed state in solution, or whether the coupling reaction of the hydroxyl-BODIPY to these polymer was incomplete.

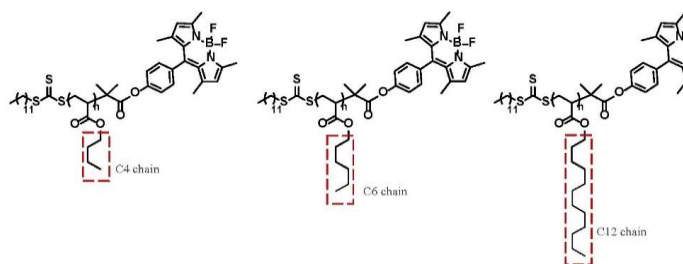


**Figure 5.** BODIPY-labelled polymers. The polymers contain BODIPY head groups with different lengths aliphatic chains; (from left to right) C4, C6 and C12, respectively.

In parallel with efforts to understand the fluorescence spectra of the polymers in chloroform, we have performed experiments characterizing their self-assembly in liquid crystal defects. Fig. 7 shows the results of an experiment using BODIPY-C4-polymer and 5CB. For a concentration of BODIPY-C4-polymer at 200  $\mu\text{M}$ , the self-assembly of the polymers in the defect were observed through the dimer signal in fluorescence microscopy, exhibiting a very thin line along the defect (indicated by red arrows in Fig. 7b). In addition to the uniform decoration of the defect, we observed that additional aggregates of polymers attached at various points along the defect. These aggregates may have formed in bulk liquid crystal, and then migrated to the defect. Upon

increasing the concentration of BODIPY-C4 to 500  $\mu\text{M}$ , we again confirmed the presence of self-associated polymers in the defect with a fine fluorescent line while observing again larger aggregates in and around the defect. Ongoing experiments are seeking to identify the origin of these bulk aggregates – it may be connected to observations reported in Figure 6.

Based on data obtained so far, the next step will be to reduce the concentration of the polymers to minimize the excess aggregates in defects and the bulk liquid crystal. This will enable us to quantify a threshold concentration of polymers

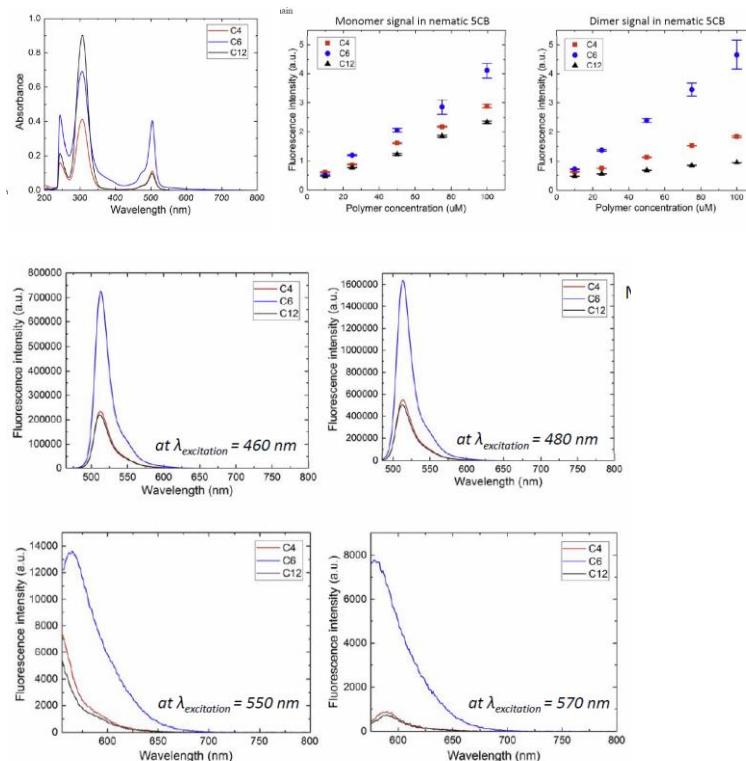


**Figure 6:** Characterization of the absorbance (top left), fluorescence intensity (top right) and emission spectra (bottom panel of four) for the DODIPY-functionalized poly(alkyl acrylate) molecules synthesized by RAFT.

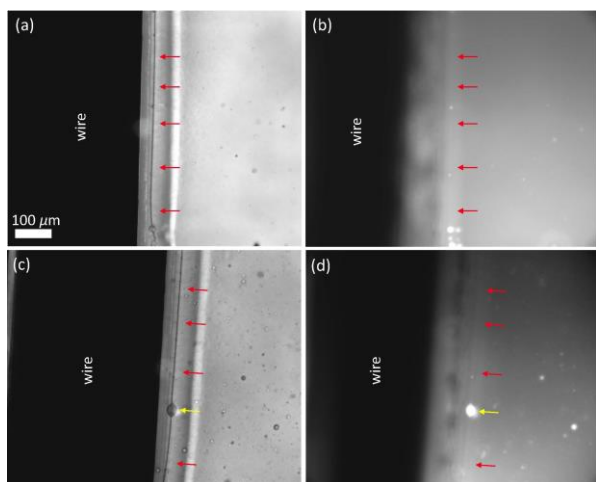


**Figure 7. Self-assembled polymers (BODIPY-C4-polymer) in defects.** (a, c) Bright-field micrographs of -1/2 disclinations (indicated by red arrows) and (b, d) fluorescence micrographs ( $\lambda_{\text{emission}}$  606-684 nm, the dimer signal of BODIPY) showing the distributed BODIPY-C4-polymer (a-b: 200  $\mu\text{M}$ , c-d: 500  $\mu\text{M}$ ) in the defects, as well as around the defects in nematic 5CB.

to cause the self-association of the polymers in defects. By precisely adjusting the concentrations, we will investigate the impact of the side chain length on the self-assembly behavior. The self-assembled polymers will be primarily studied with fluorescence microscopy, and we will seek to explore the resulting architecture in defects with transmission/scanning electron microscopy (after cross-linking of the polymeric assemblies).

**Experiments with polymerizable amphiphiles** Analogous to the previous systems, we have ongoing experiments being performed with polymerizable amphiphiles in defects of liquid crystals. Abbott gave a seminar at University of Colorado in May of 2018, and discussed with Professor Doug Gin opportunities to

use 1,3-alkyldiene gemini surfactants in studies of self-assembly of amphiphiles in liquid crystal defects (Fig. 8). Of particular interest is the polymerizable dimeric surfactant, which gives a different packing parameter from what we have investigated to date. At the same time, the gemini surfactant forms bicontinuous cubic phases resulting in interesting structures like the double diamond lattice ( $Pn3m$ ) or the gyroid lattice ( $la3d$ ) in polar solvents (e.g., water and glycerol). We are studying how changing the spacer length (carbon chain between the head groups, highlighted by yellow region in Fig. 8) influences the self-assembly behavior. By increasing the spacer length, we predict that we will be able to tune and access different packing parameters that would ultimately change preferred aggregate nanostructures. Once we have confirmed formation of polymeric assemblies in the defects, we plan to characterize the nanostructures by using with transmission/scanning electron microscopy.

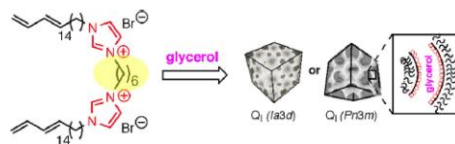


**Figure 8. An imidazolium-based gemini surfactant.** The monomeric surfactant forms crosslinkable bicontinuous cubic phases. The illustration is provided by Dr Gin.

### ***Influence of molecular self-assembly on defect dynamics in liquid crystals***

One of the key goals of our project is to understand how molecular self-assembly influences the dynamics of defect motion, with the ultimate goal of showing how macroscopic dynamics of defects can be harnessed to report formation of a single nanoscopic amphiphilic assembly. Over the past year, we have made progress towards this goal. As detailed in our proposal, the experiments are based on generating  $\pm 1$  point defects by heating 5CB into an isotropic phase and subsequently wicking it into capillaries with inner diameter (DO) of 400  $\mu\text{m}$ . The inner surfaces of the capillaries were chemically-functionalized with N,N-dimethyl-N-octadecyl-3-aminopropyl-trimethoxysilyl chloride (DMOAP) to induce perpendicular (homeotropic) anchoring of the LC director. Following filling of the capillary, the 5CB was quenched thermally into the nematic phase. This geometry results in point singularities that can be observed optically along the capillary axis at domain boundaries. Previously, we have shown that the  $\pm 1$  defects are attracted to each other due to the elasticity of the liquid crystal (Fig 9a-f). This attractive interaction acts on both defects with opposite strengths over a very large separation (several hundreds of micrometers). At separations lower than tens of micrometers, we observe the defects to optically fuse limited by optical resolution. After contacting with each other, they annihilate, resulting in a defect-free liquid crystal ordering. Fluorescence micrographs in Figs. 1g show that the molecular assemblies remain intact immediately after defect annihilation. Over the subsequent 30 min, the assemblies (of DLPC) slowly dissociated and diffused in the defect-free nematic LC, indicating that these molecular assemblies are long-lived. Representative TEM micrograph of the molecular assemblies shows toroidal-shape assemblies comprised of three periodic lipid bilayers, as shown in Fig. 9h. This observation is consistent with previous theoretical studies that predicted the core structure of  $+1$  defects to be nanoscopic closed-loop disclination.

To provide insight into the role of the molecular assemblies in defining the dynamics of defects, over the past year we derived a simple model to analyze the dynamics of defects and we have tested this model to see if changes in the sizes of assemblies formed within defects are reflected in the changes in the macroscopic dynamics of defects. To set up the model, we evaluate the elastic force driving the defects to annihilate as

$$f_{\text{defect}} = K \left( \frac{d}{d_0} \right)^{-2.9}$$

in which  $K$  is the elastic constant of the LC (using the ‘one constant’ approximation). This elastic force is opposed by a Stokes drag force, which can be written as:

$$f_{\text{drag}} = C_D v$$

in which  $C_D$  is the Stokes drag coefficient, i.e.,

$$C_D = 6\pi\mu_{\text{apparent}}a$$

where  $\mu_{\text{apparent}}$  is the apparent viscosity, and  $a$  is the effective hydrodynamic radius of the topological defects. By interpreting measurements of defect dynamics in terms of a drag coefficient or effective size ( $a$ ), we have examined how cross-linking of assemblies within defects (i.e., quenching of assembly dynamics) as well as assembly size impact defect dynamics. These

experiments were performed using the photoreactive lipid diyne PC doped with 3 % BODIPY-C5 (instead of DLPC). We found that the dynamics of  $\pm 1$  defects with 5CB/diyne PC mixture are similar to DLPC, with CAC and CSat of diyne PC  $\sim 10 \mu\text{M}$  and  $19 \mu\text{M}$ , respectively (see Fig. 10a). More importantly, crosslinking of assemblies of diyne PC neither prevented defect annihilation nor changed the dynamics of defects. This observation indicates that the internal dynamics of assemblies within the defect core do not have a significant impact on the dynamics of defects. Furthermore, based on  $C_D$  shown in Fig. 10b, we calculate the ratio of  $a_{19\mu\text{M}}^{+1, C_D} / a_{10\mu\text{M}}^{+1, C_D}$  to be  $\sim 1.34$  (i.e., that the assemblies formed from  $19 \mu\text{M}$  lipid are larger than  $10 \mu\text{M}$  lipid, by a factor to 1.34). To test this prediction based on defect dynamics, we measured independently the Brownian motion of self-assembled core in nematic 5CB with uniform homeotropic alignment, as shown in Fig. 10c. Fig. 10 shows the mean square displacement (MSD) as a function of time. The diffusion coefficient  $D$  can be calculated from the MSD. Based on the MSDs and  $D$  calculated from Fig. 10d, we

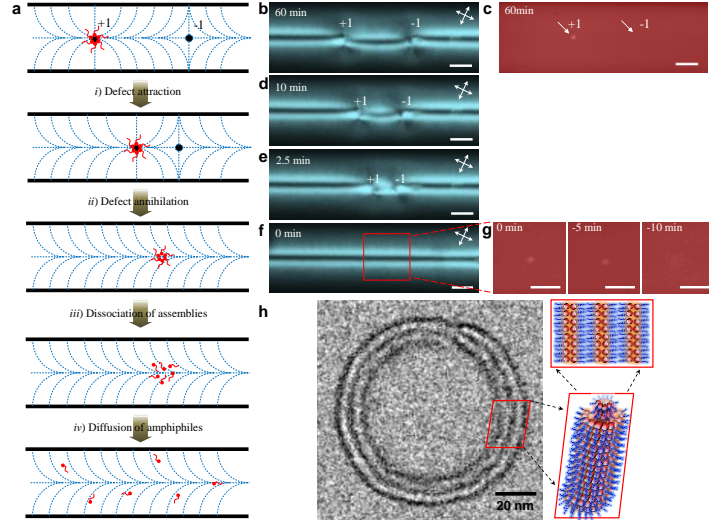


**Figure 9 Dynamics of defects and self-assembled defect cores. a,** Schematic illustration of motion and annihilation of  $\pm 1$  defects and dynamics of self-assembled defect core in a capillary filled with nematic LC. Dashed blue line illustrates local ordering of mesogens. **b,d-f,** Polarized light micrographs showing the dynamics of defects formed in a mixture of DLPC/5CB in a capillary. The white double-headed arrows indicate the orientation of the crossed polarizers. **c,g,** Fluorescence micrographs showing the temporal evolution of molecular assemblies in this process. DLPC concentration is  $57 \mu\text{M}$ . DLPC is mixed with BODIPY-C5 at 4% mol/mol based on DLPC. The times at which the micrographs were obtained (**b-f**) before or (**g**) after defect annihilation are indicated (time was set to 0 when the defects were annihilated). Scale bars,  $100 \mu\text{m}$ . **h,** Representative TEM image and schematic illustration of diyne PC assemblies templated by  $+1$  defects. Diyne PC concentration is  $19 \mu\text{M}$

calculate  $a_{19\mu\text{M}}^{+1, \text{MSD}} = 56 \pm 5$  nm and  $a_{10\mu\text{M}}^{+1, \text{MSD}} = 42 \pm 4$  nm, and thus  $a_{19\mu\text{M}}^{+1, \text{MSD}} / a_{10\mu\text{M}}^{+1, \text{MSD}} \sim 1.33$ , in close agreement with  $a_{19\mu\text{M}}^{+1, C_D} / a_{10\mu\text{M}}^{+1, C_D} \sim 1.34$ . Furthermore, the TEM images of diyne PC assemblies shown in insets in Fig. 10d lead us to calculate that  $a_{19\mu\text{M}}^{+1, \text{TEM}} = 65 \pm 5$  nm,  $a_{10\mu\text{M}}^{+1, \text{TEM}} = 50 \pm 5$  nm, and  $a_{19\mu\text{M}}^{+1, \text{TEM}} / a_{10\mu\text{M}}^{+1, \text{TEM}} \sim 1.30$ . We note here that  $a^{+1, \text{TEM}}$  is the hydrodynamic size rather than structural size. Overall, these results support our hypothesis that the molecular assemblies expand  $a^{+1}$  to slow  $v^{+1}$ . The results provide further evidence that measurements of the macroscopic motion of defects can provide insights into changes in the organization of nanoscopic assemblies that form within them. Whereas our previous measurements had shown the formation of assemblies slows defect motion, the key finding in Fig. 10 is that changes in the sizes of amphiphilic assemblies can also be transduced by measurements of defect motions.

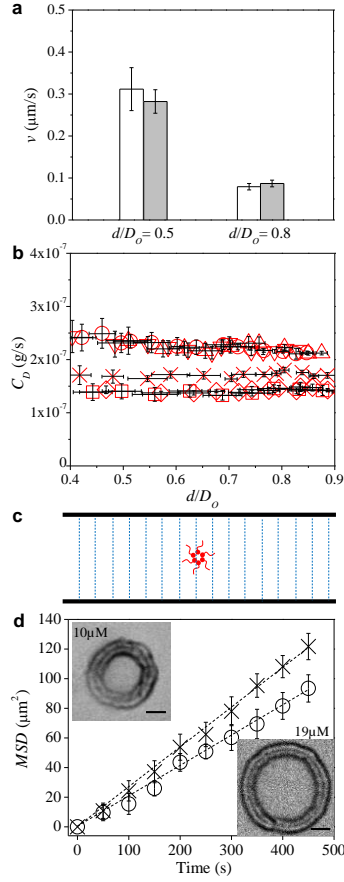


**Figure 10 Dynamics of defects in diyne PC/5CB mixture and nanostructure of self-assembled cores.** **a**,  $v^{+1}$  of (gray) uncrosslinked and (white) crosslinked self-assembled cores. **b**,  $C_D$  of +1 defects as a function of  $d$ . Pure 5CB:  $\square$ . Diyne PC:  $\diamond$  5  $\mu\text{M}$ ;  $\times$  10  $\mu\text{M}$ ;  $\circ$  19  $\mu\text{M}$ ;  $\Delta$  19  $\mu\text{M}$  (crosslinked);  $\nabla$  38  $\mu\text{M}$ . **c**, Scheme of assemblies in homeotropic anchoring LCs. Dashed blue line illustrates local ordering of mesogens. **d**,  $\text{MSD}$  of diffusion of crosslinked self-assembled cores as a function of time.  $\times$  10  $\mu\text{M}$ ;  $\circ$  19  $\mu\text{M}$ . Dashed lines represent the best-fit of the data. Insets in **(d)** show representative TEM images of diyne PC assemblies templated by +1 defects. Three assemblies at each concentration were characterized. Error bars represent standard deviations and  $n = 3$  for each data point. Scale bars, 20 nm.